A nonlinear catastrophe model of instability of planar-slip slope and chaotic dynamical mechanisms of its evolutionary process

Siqing Qin [a,*], Jiu Jimmy Jiao [b], Sijing Wang [a], Hui Long [a]

[a] *Engineering Geomechanics Laboratory, Institute of Geology and Geophysics, Chinese Academy of Sciences, PO Box 9825, Beijing 100029, People's Republic of China*
[b] *Department of Earth Sciences, The University of Hong Kong, Pokfulam Road, Hong Kong, People's Republic of China*

Abstract

This paper presents a nonlinear cusp catastrophe model of landslides and discusses the conditions leading to rapid-moving and slow-moving landslides. It is assumed that the sliding surface of the landslides is planar and is a combination of two media: one is elasto-brittle and the other is strain-softening. It is found that the instability of the slope relies mainly on the ratio of the stiffness of the elasto-brittle medium to the stiffness at the turning point of the constitutive curve of the strain-softening medium. A nonlinear dynamical model, which is derived by analyzing the catastrophe model and considering external environmental factors, is used to reveal the complicated mechanisms of the evolutionary process of the slope under environmental influence and to explore the condition of the occurrence of chaos and the route leading to chaos. The present analysis shows that, when the nonlinear role of the slope itself is equivalent to the environmental response capability, a chaotic phenomenon can occur and the route leading to chaos is realized by bifurcation of period-doublings. © 2001 Elsevier Science Ltd. All rights reserved.

Keywords: Catastrophe; Chaos; Instability; Stiffness ratio; Plane-slip slope

1. Introduction

Although great efforts (Skempton, 1985; Lan, 1993; Qin et al., 1993; Chau, 1995; Claes, 1996; Duncan, 1996) have been made in the study of slope stability, the harsh reality of failing to predict many catastrophic landslides in the world shows that so far we understand little about landslide mechanisms. A common method for evaluating the stability of a slope is the limit equilibrium analysis. The factor of safety defined by the limit equilibrium method of a rigid body is the ratio of resisting forces to driving forces. This method has a great drawback. As an example considering the planar-slip slope, it is assumed that the sliding surface

---

* Corresponding author. Tel.: +86-10-62008343; fax: +86-10-62040574.
E-mail address: qinsiqing@hotmail.com (S. Qin).

is composed of two kinds of media with different strength and that the rock mass above it is a rigid body. The total resisting force is

$$F_{\text{anti}} = \tau_{\text{f1}}L_1 + \tau_{\text{f2}}L_2 \tag{1}$$

where τ_{f1} and τ_{f2} are the peak values of shear stress for media 1 and 2, respectively, and L_1 and L_2 are the length along the sliding surface, respectively.

It is seen from the curve of the shear stress τ versus the sliding displacement u that this method is suitable only when the constitutive curves of media 1 and 2 simultaneously reach their peak stress values at some displacement value (Fig. 1). However, it is highly unlikely that the constitutive curves of two media would come to their peak stress values simultaneously (Fig. 2). Thus, the resisting force can not be calculated properly by Eq. (1). Hence, it is suggested that a new approach to evaluate the stability of a slope should be considered which allows for the displacement along the sliding surface.

In addition, there are many intriguing unanswered questions related to rainfall-induced landslides (Chau, 1995). For example, at a particular hill-side under heavy rainfall, why does one slope fail while the adjacent slopes stand, even though the rainfall data and the slope type are virtually the same? How can one
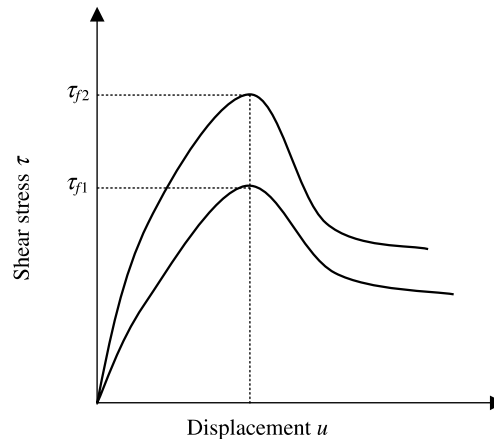

Fig. 1. Constitutive curves of the media of sliding surface, simultaneously reaching the peak stress values.
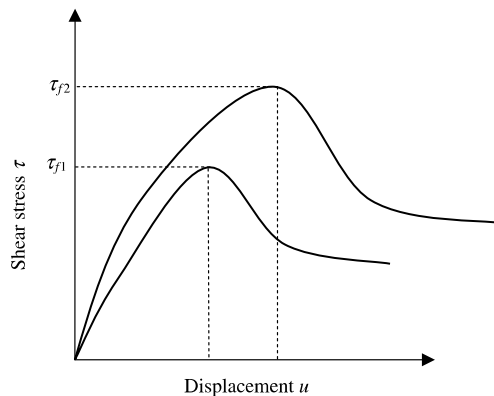

Fig. 2. Constitutive curves of the media of sliding surface, not simultaneously reaching the peak stress values.

explain that a failure occurs at a rainfall which may not be the heaviest one in the history? These questions are difficult to answer using the traditional slope stability analysis approaches. It is believed that a nonlinear dynamical model which can reflect the subtle nature of the evolution of slope failure may lead to a better prediction of landslides.

The concepts and mathematical techniques associated with nonlinear dynamical systems (NDS) theory have been widely applied in virtually every scientific discipline including rock mechanics and geology (Thom, 1972; Henley, 1976; Saunders, 1980; Keilis-Borok, 1990; Phillips, 1993; Qin et al., 1993; Phillips, 1995; Li and Huang, 1998). These concepts include chaos, fractal geometry, and catastrophe theory (Phillips, 1992). The utility of the NDS concepts and techniques in the study of a landslide brings a brilliant opportunity to make enhanced insights into the landslide mechanisms. The study of the dynamical behavior of the evolutionary process of landslides by applying NDS theory has attracted the attention of many researchers. Qin et al. (1993), Tang (1993), Tang et al. (1993), and Henley (1976) presented a few catastrophe models in their studies of slope instability, reservoir-induced earthquake, coal pillar burst, rock specimen instability and fault movement. Chau (1995, 1999) analyzed the bifurcations of a creeping slope with one-state and two-state variable friction laws. Cui (1991), Cui and Guan (1993), Yi (1995), and Chau (1998) conducted experimental studies on the mechanism and onset condition of debris flow and hence established catastrophe models of debris flow initiation. Many researchers (Phillips, 1993; Qin et al., 1993; Phillips, 1995; Li and Huang, 1998; Qin, 2000) found that chaos may appear in the evolutionary process of a slope.

Deterministic chaos results in complex, irregular patterns arising from deterministic systems (Phillips, 1995). Chaotic systems are sensitive to initial conditions and perturbations. One consequence is that small errors in the specification of the initial state can be amplified rapidly. Due to the inevitability of errors in the observational and numerical sources from which initial conditions are obtained, it is generally believed (Phillips, 1993; Qin, 2000; Qin et al., 2000) that the predictability limit (or predictable time scale) of landslides should be considered bearing in mind that the evolutionary behavior of landsliding is chaotic. Considerable speculations and some evidence indicate that chaos may be common in geophysical phenomena (Phillips, 1995; Qin, 2000; Keilis-Borok, 1990).

Are there chaotic phenomena in the evolutionary process of a slope under the influence of external environment factors? What are the conditions and routes leading to chaos? These problems have to be solved in order to make a better evaluation of the stability of a slope and more accurate prediction of a landslide.

Catastrophe theory is a mathematical technique developed principally by Thom (1972) for modeling natural phenomena which contain discontinuities and sudden changes in the values of one or more parameters. Most landslides can be regarded as a discontinuous catastrophe phenomenon. Thus, it is appropriate to use catastrophe theory to study landslides. In this paper, we will study the unstable mechanisms of a planar-slip slope, in which sliding-surface materials comprise two kinds of media: one is elasto-brittle and the other is strain-softening. Using catastrophe theory, the conditions leading to a rapid-moving landslide and a slow-moving landslide (creeping landslide) will be presented. To analyze the environmental impact on the evolutionary process of a slope, a nonlinear dynamical model will be presented to reveal the root of complexity of landslide evolution and to explore the condition leading to chaos.

2. Analysis on the unstable process of planar-slip slope by catastrophe theory

2.1. Mechanical model

It is assumed that the sliding surface with the dip β is a nonuniform intercalation and that the rock mass above it is a rigid body (Fig. 3). H, mg (g is gravity acceleration) and h are the vertical height of rock mass, the weight of rock mass and the layer thickness of the intercalation, respectively. Under the action of the
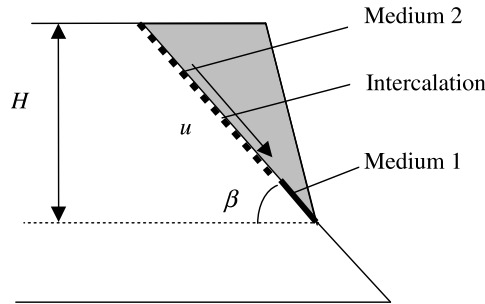
Fig. 3. Mechanical model of a planar-slip slope.

driving force caused by the weight of rock mass, the creeping displacement is u along the intercalation. Due to higher strength of the media (referred to as interfacial materials, such as rock bridge) or lower shear stress at some segments of the intercalation, the media may have an elastic or strain-hardening property. However, owing to discontinuous media, weathering and softening effect of water or higher shear stress at the other segments, the media may have a strain-softening property after the peak stress. To simplify the analysis and focus on the physical essence of the instability problem, we assume that the intercalation is composed of only two kinds of media with different mechanical properties (Fig. 3), i.e., one (medium 1) is elasto-brittle, and the other (medium 2) has a strain-softening property.

The constitutive equation for medium 1 can be assumed as

$$\tau = \begin{cases} G_e u/h & (u \leqslant u^*) \\ \tau_m & (u > u^*) \end{cases} \tag{2}$$

where G_e is the shear modulus, u^* is the critical displacement of the unstable point, and τ_m is the residual shear strength.

For medium 2, the simplified constitutive equation can be generally expressed as a nonlinear function of the shear stress τ and the creeping displacement u. Tang et al. (1993) and Qin et al. (1993) used a Weibull distribution and a negative exponential distribution of strength to describe the strain-softening property of media, respectively. In this paper, a negative exponential distribution, defined by Eq. (3), is used, but other distribution functions can also be used depending on one's understanding of the material property.

$$\tau = G_s \frac{u}{h} e^{-u/u_0} \tag{3}$$

where G_s is the initial shear modulus and u_0 is the displacement value at the peak value of the stress (Fig. 4). It is evident from Eq. (3) that $u_1 = 2u_0$ and slope $= -G_s e^{-2}/h$ at the turning point of the curve.

2.2. Cusp catastrophe model

For the system shown in Fig. 3, the overall potential energy is equal to the sum of the strain energy and driving potential energy, i.e.

$$V = l_s \int_0^u \frac{G_s u}{h} e^{-u/u_0} \, du + \frac{1}{2} \frac{G_e l_e}{h} u^2 - mgu \sin \beta \tag{4}$$

where l_e and l_s are the length of the sliding surface for media 1 and 2, respectively, and $l_s + l_e = H/\sin \beta$; u can be regarded as the state variable in the cusp catastrophe analysis. It is assumed here that l_s and l_e are far larger than u and approximately remain unchanged during sliding.
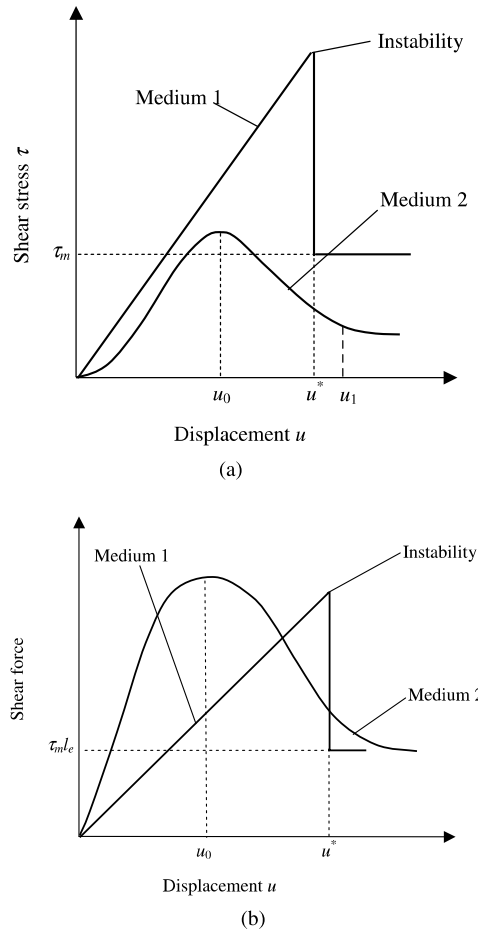
Fig. 4. Constitutive curves of two kinds of media in the intercalation. (a) Shear stress versus displacement. (b) Shear force versus displacement when the length of medium 1 with elasto-brittle property is far less than the length of medium 2 with strain-softening property.

Let $V' = 0$ and the equilibrium surface equation (Fig. 5) is expressed as

$$V' = \frac{G_s l_s}{h} u e^{-u/u_0} + \frac{G_e l_e}{h} u - mg \sin \beta = 0 \tag{5}$$

Eq. (5) is the equilibrium condition of forces. The cusp can be solved by the smoothness property of the equilibrium surface. At cusp, $V''' = 0$, i.e.

$$V''' = \frac{G_s l_s}{h u_0} (u/u_0 - 2) e^{-u/u_0} = 0 \tag{6}$$

which leads to

$$u = u_1 = 2u_0 \tag{7}$$

Eq. (7) shows that the displacement value at cusp is exactly the displacement value at the turning point of the constitutive curve of medium 2.
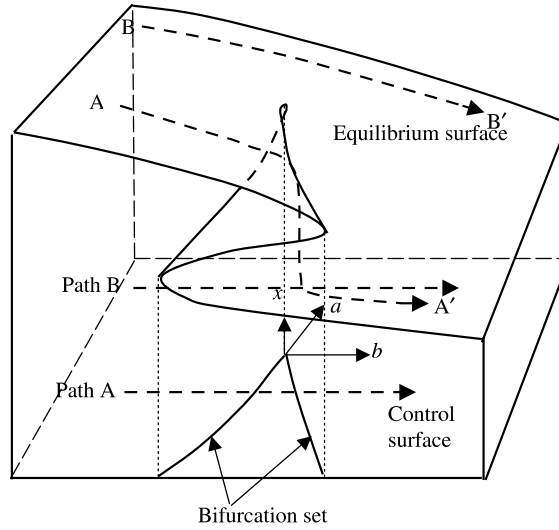
Fig. 5. Cusp catastrophe model.

Making Taylor series expansion with respect to u_1 for Eq. (5), discarding all the terms but the first three because the third order item is the minimum one away from zero while $G_e l_e e^2 / G_s l_s \to 1$ and $(1 + G_e l_e e^2 / G_s l_s) \to mghe^2 \sin \beta / G_s l_s u_1$, and substituting Eq. (6) into Eq. (5), one has

$$\frac{2}{3} \frac{G_s l_s u_1 e^{-2}}{h} \left[\left(\frac{u - u_1}{u_1} \right)^3 + \frac{3}{2} \left(\frac{G_e l_e e^2}{G_s l_s} - 1 \right) \left(\frac{u - u_1}{u_1} \right) + \frac{3}{2} \left(1 + \frac{G_e l_e e^2}{G_s l_s} - \frac{mghe^2 \sin \beta}{G_s l_s u_1} \right) \right] = 0 \qquad (8)$$

In order to transform Eq. (8) into a standard form of cusp catastrophe, let

$$x = (u - u_1)/u_1 \qquad (9)$$

$$a = 3(k - 1)/2 \qquad (10)$$

$$b = 3(1 + k - k\xi)/2 \qquad (11)$$

$$k = G_e l_e e^2 / G_s l_s \qquad (12)$$

$$\xi = mgh \sin / G_e l_e u_1 \qquad (13)$$

where k is the ratio of the stiffness of medium 1 ($k_e = G_e l_e / h$) to the stiffness at the turning point of the constitutive curve of medium 2 ($k_s = | - G_s l_s e^{-2} / h |$) (for simplicity, it is called hereafter the stiffness ratio); ξ is relative to the weight of rock mass, geometric size of the system, and mechanical parameters of media (referred to as the geometric-mechanical parameter).

Substituting Eqs. (9)–(13) into Eq. (8) leads to

$$x^3 + ax + b = 0 \qquad (14)$$

Eq. (14) is the standard cusp catastrophe model of the equilibrium surface, with a and b as its control parameters and x as its state variable.

The cusp catastrophe described by the equilibrium surface containing fold or pleat is illustrated in Fig. 5 where axes of three-dimensional space are the control parameters a, b (horizontal) and response parameter

x (vertical). The action over the equilibrium surface occurs as a smooth or catastrophic movement along the equilibrium sheet. For example, Point B undergoes action and smoothly moves to Point B′ down the equilibrium sheet representing a decrease in potential, but Point A may encounter the edge of the fold where a slight change in the parameters (trigger) causes a fall or catastrophic jump to the lower equilibrium sheet at A′. A control surface is the surface defined by the control parameters or projection of a three-dimensional equilibrium surface to a two-dimensional control space. The line that marks the edges of the pleat in the equilibrium surface, where the top and bottom sheets fold over to form the middle sheet, is called the fold curve or singularity set. When it is projected back onto the plane of the control surface, the result is a cusp-shaped curve. The singularity set can be determined from

$$V'' = 3x^2 + a = 0 \tag{15}$$

The cusp (bifurcation set) defined by the projection of the fold in the control surface determines the area of the catastrophic behavior, i.e., if the trajectory of the action passes through the cusp, a catastrophic action will occur. Combining Eqs. (14) and (15) and eliminating x, the bifurcation set can be derived as

$$4a^3 + 27b^2 = 0 \tag{16}$$

It is known from Eqs. (10) and (11) that the control parameters a and b of the system are wholly determined by the stiffness ratio k and the geometric-mechanical parameter ξ. In other words, the bifurcation set leading to catastrophe is related to the properties of the mechanical system itself and is irrelevant to external action.

Substituting Eqs. (10) and (11) into the bifurcation set equation (16), one has

$$2(k-1)^3 + 9(1 + k - k\xi^2) = 0 \tag{17}$$

The bifurcation set (Fig. 5) defines the thresholds where sudden changes can take place. As long as the state of the system remains outside the bifurcation set, the behavior varies smoothly and continuously as a function of the control parameters. Even on entering the bifurcation set no abrupt change is observed. When the control point passes all the way through the bifurcation set, however, a catastrophe is inevitable. Thus, Eq. (17) is the sufficient and necessary mechanical criteria for the planar-slip slope instability (rapid-moving landslide).

Apparently, only when $a \leqslant 0$, the condition of Eq. (16) may be satisfied, i.e., a catastrophe probably occurs. Thus, in terms of $a \leqslant 0$, the necessary condition of instability is

$$k \leqslant 1 \tag{18}$$

Eq. (18) shows that the smaller the stiffness of medium 1 is, the larger the post-peak stiffness (the absolute value of constitutive curve slope after the peak stress) of medium 2, and the more possible it is for the slope system to lead to catastrophe. Because the stiffness ratio depends on the geometric size and the material property of the system, the necessary condition leading to catastrophe is only related to the inner characteristics of the system. If the media of the intercalation are wholly hardening or if one medium is elastic and the other is ideally plastic, then $k \to \infty$ and a landslide will not occur.

Eq. (14) or (15) can be used to determine the critical displacement value of the unstable points as follows:

$$u^* = u_1 \left[1 - \frac{\sqrt{2}}{2}(1-k)^{1/2} \right] \tag{19}$$

It should be noted that, in the derivation of Eq. (19), the minus sign in front of the square-root term is used, because the state variable u or x has a jump while the landslide system passes through the left branch ($b < 0$) of the bifurcation set (Fig. 6). Eq. (19) indicates that the points of instability associated with the stiffness ratio can appear before ($k < 0.5$) or after ($k \geqslant 0.5$) the stress peak value.
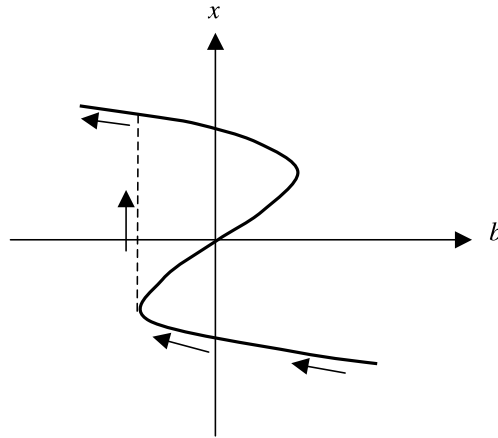
Fig. 6. A jump of the state variable x when the system passes through the bifurcation set.

When $2(k-1)^3 + 9(1+k-k\xi^2) > 0$, the slope is in a very stable state because Eq. (4) (potential function) only has a minimum value.

When the control parameters satisfy

$$2(k-1)^3 + 9(1+k-k\xi^2) < 0 \quad (k < 1) \tag{20}$$

it is shown (Saunders, 1980; Qin et al., 1993) that, although the slope body is in a limit equilibrium state under the action of internal and external factors, very small changes of these factors result in very small changes of the equilibrium states. This corresponds to a creeping landslide (slow-moving landslide).

2.3. Comparison with the limit equilibrium method

Eq. (17) can be further expressed as

$$\frac{G_s l_s}{mgh \sin \beta} = \frac{0.5 e^2}{u_0 \left[1 + k \pm \frac{\sqrt{2}}{3}(1-k)^{3/2}\right]} \quad (k \leqslant 1) \tag{21}$$

For a rapid-moving landslide, $b < 0$. Taking a plus sign for the right-hand side of Eq. (21), one obtains

$$\frac{G_s l_s}{mgh \sin \beta} = \frac{0.5 e^2}{u_0 \left[1 + k + \frac{\sqrt{2}}{3}(1-k)^{3/2}\right]} \quad (k \leqslant 1) \tag{22}$$

The factor of safety defined by the ratio of the resisting force to the driving force at certain deformation u is

$$K = \frac{G_s l_s u e^{-u/u_0} + k G_s l_s e^{-2} u}{mgh \sin \beta} = \frac{0.5 e^2 (e^{-u/u_0} + k e^{-2}) u}{u_0 \left[1 + k + \frac{\sqrt{2}}{3}(1-k)^{3/2}\right]} \tag{23}$$

It is evident from Eq. (23) that the factor of safety depends only on k and u/u_0, that is to say, K is related to the creeping displacement u.

When a slope evolves to the critical state, i.e., $u = u^*$, substituting Eq. (19) into Eq. (23), one can obtain the critical factor of safety as follows:

$$K_c = \frac{\left[1 - \sqrt{2}(1-k)^{1/2}/2\right]\left(e^{\sqrt{2(1-k)}} + k\right)}{1 + k + \frac{\sqrt{2}}{3}(1-k)^{3/2}} \qquad (24)$$

It can be seen that K_c is only related to k. The relation between K_c and k from Eq. (24) is listed in Table 1. It is seen from Table 1 that when $k = 0$, K_c is the smallest, and then K_c increases as k increases. This shows that the different stiffness ratios correspond to different critical factors of safety and that the critical factor of safety is not a fixed value of 1, as defined by the traditional equilibrium method. Thus, the limit equilibrium method is analogous to the condition $k = 1$, and is a special case of Eq. (24).

The condition leading to a slow-moving landslide can be derived from Eq. (20) for different stiffness ratios. Its expression is

$$\frac{\left[1 - \sqrt{2}(1-k)^{1/2}/2\right]\left(e^{\sqrt{2(1-k)}} + k\right)}{1 + k + \frac{\sqrt{2}}{3}(1-k)^{3/2}} < K_c < \frac{\left[1 - \sqrt{2}(1-k)^{1/2}/2\right]\left(e^{\sqrt{2(1-k)}} + k\right)}{1 + k - \frac{\sqrt{2}}{3}(1-k)^{3/2}} \qquad (25)$$

The relation between K_c and k from Eq. (25) is listed in Table 2.

It can be seen that when $k < 1$, even if the factor of safety is more than 1 but less than the critical upper-limit value listed in Table 2, we can only judge that a rapid-moving landslide will not occur, although a slow-moving landslide will inevitably take place. Thus, the limit equilibrium method can be only used to determine whether a rapid-moving landslide will occur or not. For this reason, it is apparent that slow-moving landslides can still occur even when the factor of safety calculated by the limit equilibrium method is >1.

We can also deduce that even if $K_c < 1$, but K_c is still greater than a certain value, the rapid-moving landslide may not occur. For example, when $k = 0$, $0.82 < K_c < 1$, a rapid-moving landslide will not occur. Thus, it is apparent why some slopes are still stable when $K_c < 1$. This means that a slow-moving landslide may occur, but during the slow sliding process, the landslide may be affected by external environment factors and hence re-stabilize.

It should be also noted that the evolutionary path of a slope may be changed by the action of environment factors, so that a slow-moving landslide may be turned into a rapid-moving landslide.

It is concluded from Eqs. (17) and (18) that instability of the slope relies mainly on the stiffness ratio k, not on the strength.

Table 1
Condition leading to a rapid-moving landslide

k	0	0.2	0.4	0.6	0.8	1.0
K_c	0.8187	0.8949	0.9471	0.9793	0.9956	1.0

Table 2
Condition leading to a slow-moving landslide

k	K_c
0	0.8187–2.2791
0.2	0.8949–1.5948
0.4	0.9471–1.2986
0.6	0.9793–1.1371
0.8	0.9956–1.0434
1.0	1.0

2.4. Instability mechanisms of slope

Eq. (12) shows that the stiffness ratio is related to both the shear modulus and the length of media 1 and 2 along the sliding surface. Obviously, the condition of the stiffness ratio <1 is easily satisfied for an actual slope when l_e is far less than l_s. In the following discussion, we assume that l_e and l_s remain unchanged and the stiffness ratio is in the neighborhood of $k \geqslant 1$ for analyzing the mechanisms of instability while the mechanical parameters vary under the action of water.

It is generally believed that the instability of a slope has a close connection with the action of water. Under the action of water, the shear modulus of medium 1 with an elasto-brittle property becomes lower and its shear resistance also decreases at the same time. Thus, the stress borne by medium 2 with a strain–softening property correspondingly increases and its strength also becomes lower owing to the action of water. This interaction readily makes medium 2 deform into its post-peak strain–softening phase.

After evolving into the strain-softening phase, the action of water makes the post-peak stiffness of medium 2 at the turning point increases (i.e., the steeper the curve of τ–u after peak stress value) (Fig. 7(a)) and the stiffness of medium 1 decrease. On the other hand, the post-peak stiffness of medium 2 can also increase while the drained condition becomes expedite due to progressive failures within the intercalation (Fig. 7(b)). This may result in a stiffness ratio of <1 and trigger instability of the slope. It can also be seen
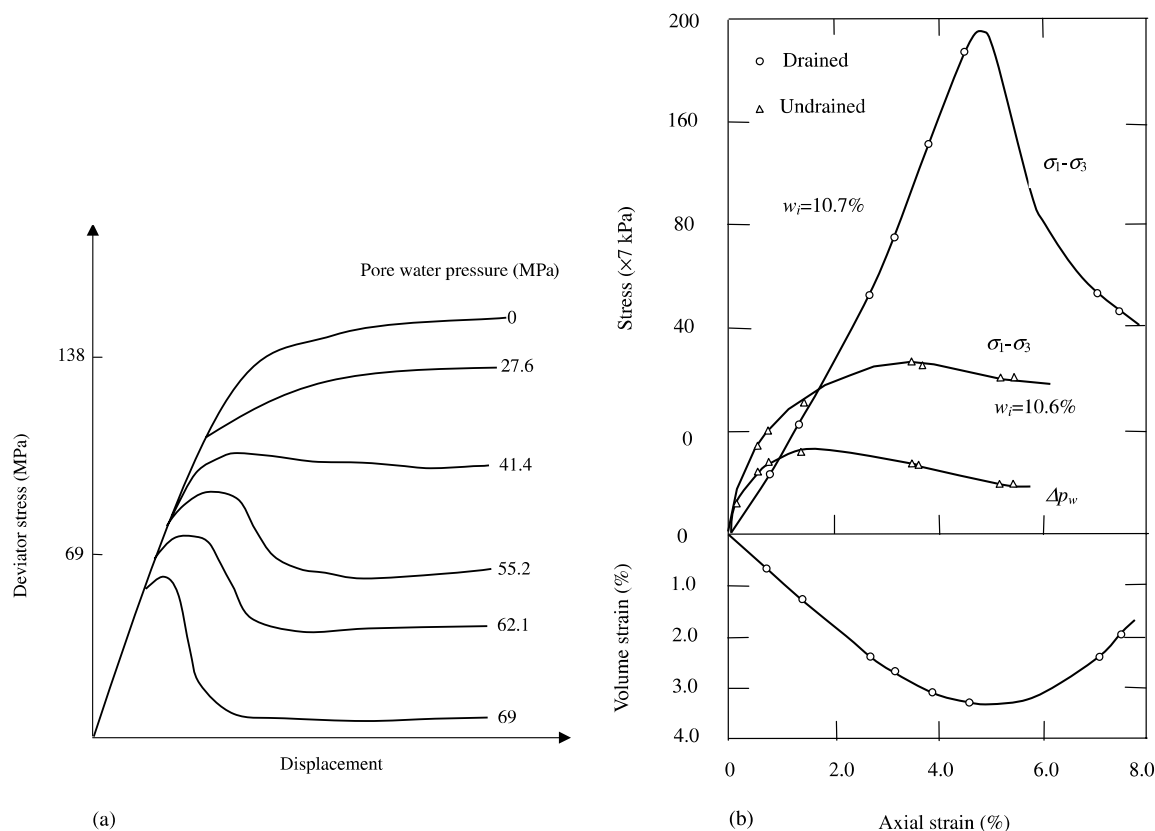

Fig. 7. (a) The effect of pore pressure on the brittle-ductile transition in limestone at a confining pressure of 6.9 MPa. Numbers on the curves are values of pore pressure in MPa (Fig. 8.9.2 in Ref. Jaeger (1979).) (b) Drained and undrained triaxial compression test results for a shale of Pennsylvanian age; w_i is the initial water content; p_w is the pore water pressure (Fig. 3.17 in Ref. Goodman (1989).)

that the larger the post-peak stiffness of medium 2, the more quickly its resistance to deformation falls at a certain displacement increment, and the higher the shear stress on medium 1 (rock bridge). This will cause the rock bridge to fail, resulting in landsliding.

3. Nonlinear dynamical model of evolutionary process of slope

In the above analysis, we considered the quasi-static movement process of the slope, but not the dynamical process of instability and the influence of external environmental factors on the evolutionary process of the slope. A nonlinear dynamical model of instability of the slope may be considered to study these problems.

The nonequilibrium resultant force leading to instability of the slope can be derived from Eq. (4)

$$F = -\frac{\partial V}{\partial u} = -c(x^3 + ax + b) \tag{26}$$

where $c = 2G_s l_s u_1 e^{-2}/3$. The expression $F = mu_1\ddot{x}$ is valid for a block to slide along a smooth inclined plane. However, for an actual planar-slip slope system, natural or artificial damped factors, such as variation of shear stress with the displacement rate $\dot{x}$ caused by the roughness of the sliding surface, should also be considered. According to Newton's viscosity law (Skempton, 1985; Qin, 2000), it is assumed that the damped force produced by damped factors is $\mu u_1 \dot{x}$. In addition, the influence of the change of environmental factors, such as four-season climate, temperature, rainfall, earthquake and vibration, on the evolutionary process of a slope, should be taken into account. Assuming that the environmental impact is a periodic force (or signal), which can be expressed approximately as $A\cos\omega t$, one has

$$F = mu_1\ddot{x} + \mu u_1\dot{x} - A\cos\omega t \tag{27}$$

where μ is the damped coefficient; A and ω are the amplitude and the circular frequency of the periodic force, respectively.

Substituting Eq. (26) into Eq. (27) leads to

$$mu_1\ddot{x} + \mu u_1\dot{x} + cx^3 + cax + cb = A\cos\omega t \tag{28}$$

Let $\mu/m = \eta$, $ca/mu_1 = \omega_0^2(a > 0)$, $\alpha = c/mu_1$, and $p = A/mu_1$. Considering that the constant item (cb/mu_1) has a very small impact on the evolutionary behavior of nonlinear equation (28), we can neglect the constant item in order to focus on the essence of the instability problem. Eq. (28) can be rewritten as

$$\ddot{x} + \eta\dot{x} + \alpha x^3 + \omega_0^2 x = p\cos\omega t \tag{29}$$

where α represents the nonlinear mechanical property of the system under the influence of rainfall or earthquake. Eq. (29) is similar to the Duffing's equation (Homes and Rand, 1976; Liu, 1995).

Because the external load $p\cos\omega t$ varies with a simple harmonic oscillation, the solution of Eq. (29) (Homes and Rand, 1976) is assumed to be in the following form

$$x = W\cos(\omega t + \phi) \tag{30}$$

where W is the amplitude and ϕ is the initial phase.

Substituting Eq. (30) into Eq. (29), neglecting the third order harmonic item, and using the condition of coefficients prior to $\cos\omega t$ and $\sin\omega t$ being zero, one obtains

$$W^2\left(\omega_0^2 - \omega^2 + \frac{3}{4}\alpha W^2\right)^2 + W^2\eta^2\omega^2 = p^2 \tag{31}$$

Eliminating the second order item on W^2 of Eq. (31) leads to

$$(B + Q)^3 + (B + Q)u_{\mathrm{d}} + v_{\mathrm{d}} = 0 \tag{32}$$

where

$$B = W^2 \tag{33}$$

$$\rho = \omega_0^2 - \omega^2 \tag{34}$$

$$Q = 8\rho/9\alpha \tag{35}$$

$$u_{\mathrm{d}} = 16(3\eta^2\omega^2 - \rho^2)/27\alpha^2 \tag{36}$$

$$v_{\mathrm{d}} = -16\{8\rho(\rho^2 + 9\eta^2\omega^2) + 81\alpha p^2\}/729\alpha^3 \tag{37}$$

where $B \pm Q$ is the state variable; u_{d} and v_{d} are the control parameters. Eq. (32) (Homes and Rand, 1976) is the standard equilibrium surface equation of double cusp catastrophe (Fig. 8), because the state variable itself is composed of variables B and Q. The position of two cusps can be solved by $u_{\mathrm{d}} = 0$ and $v_{\mathrm{d}} = 0$. Let $f = \omega^2 - \omega_0^2 = -\rho$, and the following solutions can be obtained:

$$f_{1,2} = 3\eta\left(\frac{\eta}{2} \pm 2\sqrt{\frac{9}{4}\eta^2 + 3\omega_0^2}\right) \tag{38}$$

$$\alpha_{1,2} = \frac{32f_{1,2}^2}{81p^2} \tag{39}$$

The coordinates of two cusps in Fig. 8 are O_1 (f_1, α_1) and O_2 (f_2, α_2), respectively.

In fact, $f(f = \omega^2 - \omega_0^2)$ is the quadratic error between the oscillation frequency ω of input signals of the external environment and the self-oscillation frequency ω_0 of the system. For simplicity, it is referred to as
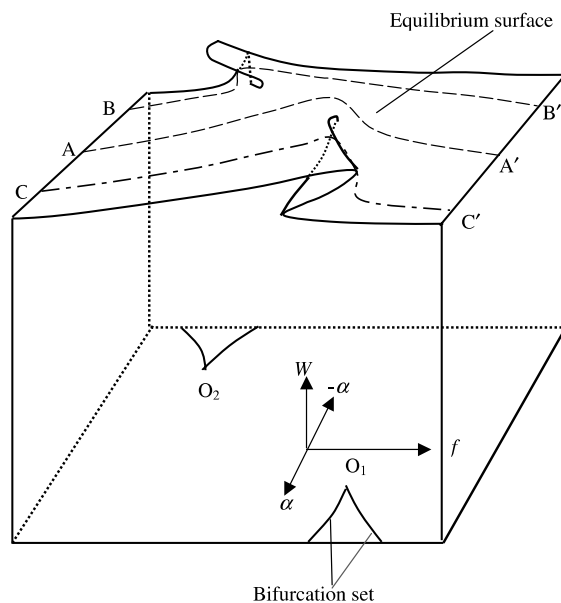

Fig. 8. Catastrophe model with double cusps.

the frequency difference. Fig. 8 shows the relation among the amplitude W, the frequency difference f and the nonlinear coefficient α. The following is an analysis of the effect of different values of α on the dynamical system:

(1) When α is a minuscule value and can be neglected, i.e., the nonlinear property of the oscillation system is very weak, the oscillation system mainly behaves like a linear vibrator. The following equation can be derived from Eq. (31)

$$W = \frac{p}{\sqrt{(\omega_0^2 - \omega^2)^2 + \eta^2 \omega^2}} \tag{40}$$

Eq. (40) shows that when the oscillation frequency ω of the environmental signal is close to the self-oscillation frequency ω_0 of the system, the amplitude of the system increases and so-called resonance phenomenon appears (path AA' in Fig. 8).

(2) When $\alpha < \alpha_2$, the position of the maximum amplitude value is not at that of $\omega \to \omega_0$, but is within some frequency range of $\omega < \omega_0$ (path BB' in Fig. 8).

(3) When $\alpha > \alpha_1$, the position of the maximum amplitude value is in the frequency range of $\omega > \omega_0$ (path CC' in Fig. 8).

The above analysis shows that when $\alpha \neq 0$, i.e., the nonlinear property of the system is considered, the influence of the environmental factors on the slope stability is very complicated. In other words, the time for the landslide to occur is possibly not synchronous with the period of rainfall or earthquake, possibly explaining the delayed response of slope movements to rainfall (Chau, 1995). This may also explain the difficulties experienced in trying to establish a statistical relation between rainfall data and landslide occurrence.

4. Chaotic effects produced by the nonlinear dynamical model

Chaos is one of the characteristics of the nonlinear system. A very small change of initial conditions may lead to a great response of the system. This response is obviously uncertain. Eq. (28) indicates that chaos may appear in the evolutionary process of a slope.

Assume that all the parameters are constants except $p = A/mu_1$ in Eq. (28). For simplicity, let $\mu/m = 0.3$, $ca/mu_1 = -1(a < 0)$, $c/mu_1 = 1$, $cb/mu_1 = 0$, and $\omega = 1.2$. Thus, Eq. (28) becomes

$$\ddot{x} + 0.3\dot{x} + x^3 - x = p \cos 1.2t \tag{41}$$

The solutions of Eq. (41) for different values of p are shown in Fig. 9. When $p < 0.3$, all solutions of $x(t)$ are periodically oscillating and the periods doubly increase in turn. When $p = 0.2$, the oscillating period τ is equal to the period T of the external environmental signal, i.e., $\tau = T = 2\pi/1.2$. When $p = 0.27$, 0.28, and 0.2867, $\tau = 2T$, $\tau = 2^2T$, and $\tau = 2^3T$, respectively. When p increases continuously and reaches the critical value $p_\infty (p_\infty \approx 0.3)$, τ is 2^∞. In other words, the period becomes infinite, i.e., the system does not hold periodicity any more and chaos appears. This means that when the magnitude of the external environmental signals gradually become enhanced, chaos can appear in the evolutionary process of a slope and its route leading to chaos is realized by the bifurcation of period-doublings.

When the values of p are within the range of chaos, there exists a narrower periodic window, as illustrated in Fig. 9(f) between (e) and (g). The period in Fig. 9(f) is $5T$. As the values of p increase within the chaotic interval, the periodic oscillation with period 2^nT may appear ($n = \ldots, 2, 1, 0$), such as the oscillation with periods $2T$ and $1T$ in Fig. 9(h) and (i). This shows that under the environmental influence, the evolutionary behavior of a slope is a complex nonlinear process: sometimes periodical and sometimes chaotic. If the evolutionary behavior of a slope is periodic, a deterministic prediction can be made; if it is chaotic,
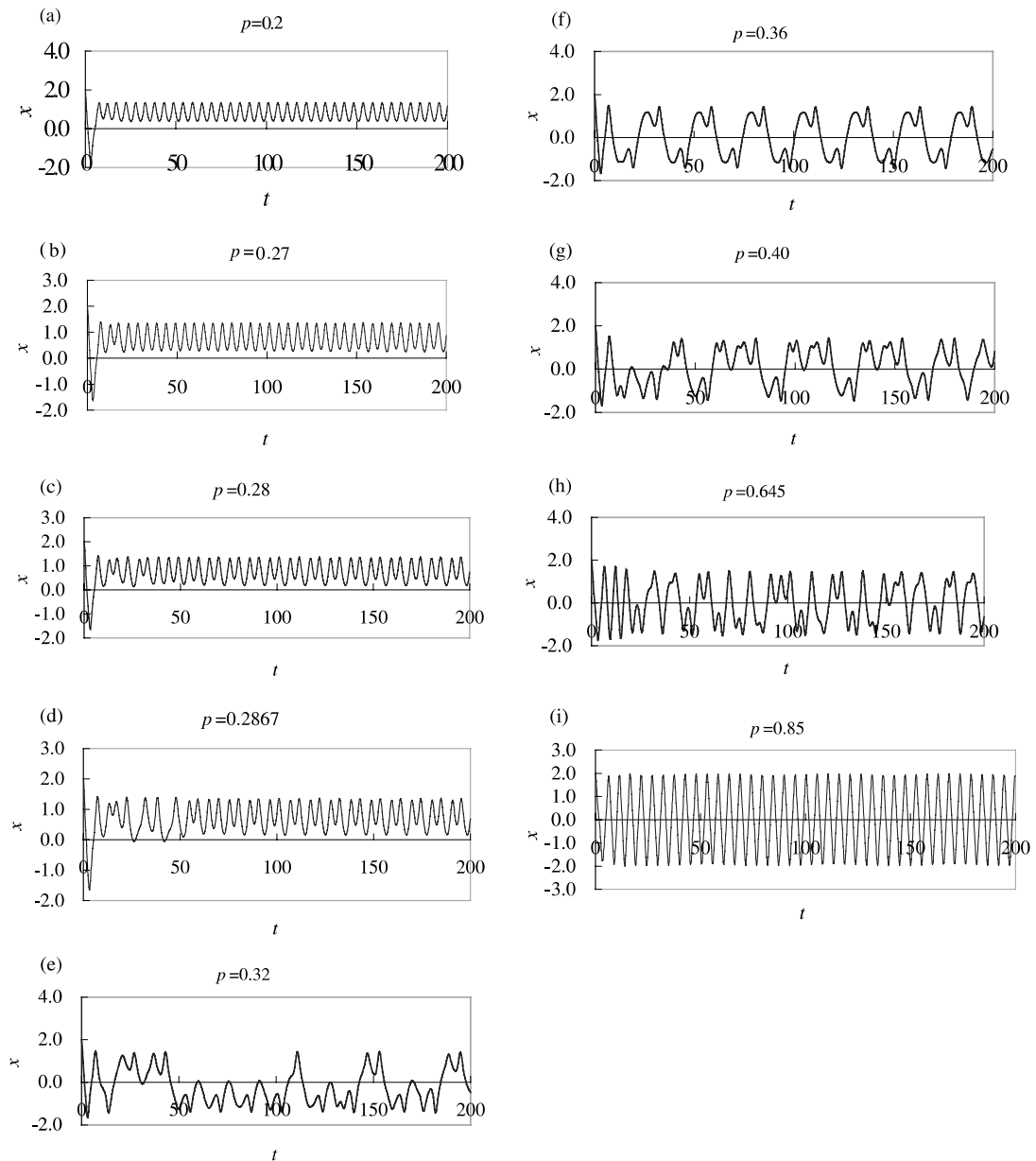
Fig. 9. Curves of x–t for different values of p (p = 0.20, 0.27, 0.28, 0.2867, 0.32, 0.36, 0.40, 0.645, 0.85).

the predictable time scale (Qin et al., 2000) must be considered and the accuracy of prediction during the time scale should be studied. The above analysis also indicates that chaos can be produced by a deterministic model and the occurrence of chaos lies in the interaction between the nonlinear properties of the slope itself and the environmental factors.

The phenomenon of period-doubling oscillation (or bifurcation) leading to chaos can be also seen from the trajectory in phase plane$(x, \dot{x})$. Fig. 10 represents the trajectory in the phase plane corresponding to
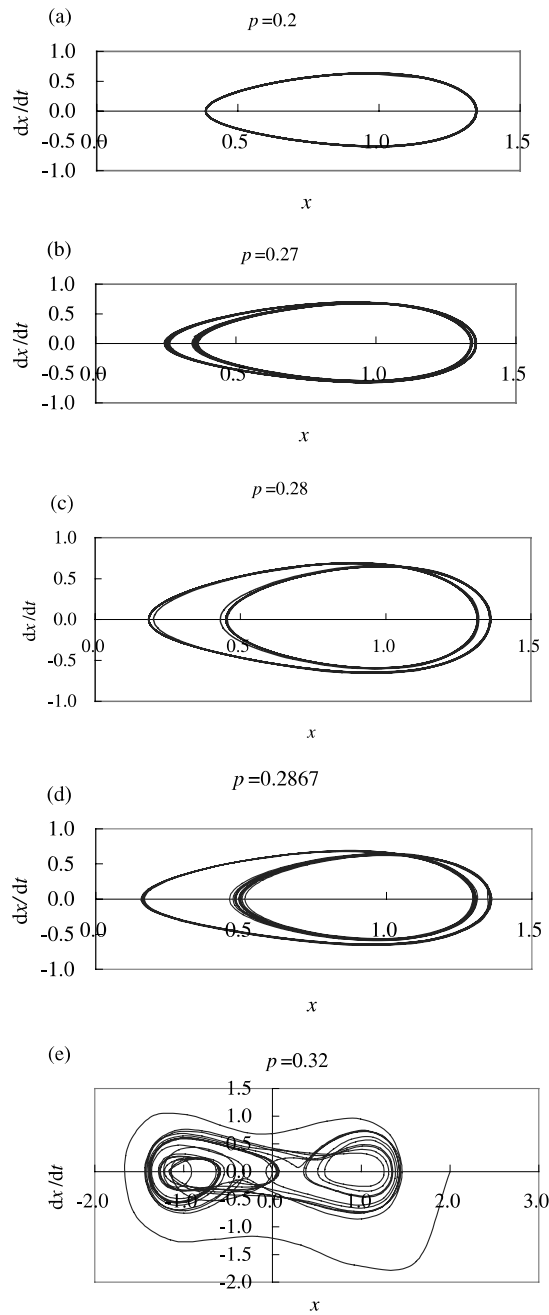
Fig. 10. Trajectories of $(x, \dot{x})$ for different values of p.

Fig. 9(a)–(e) (transient-state process is removed). It can be seen that periodic motions are all along closed curves. The periodic oscillation with period $2^n T$ has n trajectories with a similar trend, and these trajectories have n points of intersections. As for chaotic motion (Fig. 10(e)), it can be seen that its trajectory is dis-

ordered. However, this does not imply that the chaotic motion is wholly disordered and does not have a certain structure. In fact, it has an inner structure. Here, we suggest to use the following method to analyze such a complex motion.

The forced vibration system can be seen as the coupling of two oscillation subsystems: one is Duffing equation

$$\ddot{x} + 0.3\dot{x} + x^3 - x = 0 \tag{42}$$

which represents the nonlinear subsystem, and the other is the periodic force acted by external environmental factors, which can be regarded as a linear simple harmonic oscillating subsystem. It is evident that Eq. (42) has three singular points (Liu, 1995): (1) saddle point: $x_1 = 0$ and $x_2 = 0$; (2) stable spiral point: $x_1 = 1$ and $x_2 = 0$; and (3) stable spiral point: $x_1 = -1$ and $x_2 = 0$. When the amplitude p of the periodic force is relatively small, the oscillation of the linear subsystem and its role on the nonlinear subsystem are very weak, and the motion of the whole system is oscillating around one of two stable spiral points of the nonlinear subsystem with the frequency ($\omega = 1.2$, $\tau = T$) of the linear vibrator (Fig. 10(a)). When p increases slightly, the impact of the nonlinear subsystem is to make the oscillation of the whole system produce fractional frequency (period-doublings) around the stable spiral point (Fig. 10(b)). When p increases further and exceeds the interval among three singular points, the system can bounce and oscillate among these singular points back and forth (Fig. 10(e)), then the motion becomes more complicated, and chaos emerges. When p increases more significantly, the linear vibrator holds a dominant role. At this time, the role of the nonlinear subsystem is relatively weak, and the whole system moves in a pattern of the linear subsystem. This means that the whole system is locked at the frequency of the periodic force ($\tau = T$). In summary, when one of two coupling subsystems plays a dominant role, the whole system is in the state of period-doublings. Only when the interacting capability of two subsystems is matched, two oscillations have a strongly mutual impact and chaos emerges. The above analysis shows that the chaotic phenomenon can appear when the nonlinear role of the slope itself is equivalent to the response capability of the linear periodic force produced by the external environmental factors.

5. Conclusions

The following conclusions are obtained from the above analysis:

1. A cusp catastrophe model of a planar-slip slope, whose sliding surface is composed of two kinds of media (medium 1 is elasto-brittle and medium 2 is strain-softening), is presented based on catastrophe theory. The conditions leading to a rapid-moving landslide and a slow-moving landslide are also derived. It is found that the instability of the slope relies mainly on the ratio of the stiffness of medium 1 to the post-peak stiffness of medium 2. The critical factor of safety varies with the stiffness ratio and is not a fixed value of 1, as defined by the traditional limit equilibrium method.

2. A nonlinear dynamical model of the evolutionary process of slope is presented by making further analysis on the catastrophe model. It is found that the relation between the external environmental factors and the response of the slope system is complexly nonlinear. This means that the occurrence time of a landslide is probably not synchronous with the maximum rainfall or earthquake.

3. When the nonlinear role of the slope itself is equivalent to the response capability of the external environmental factors, chaos can appear in the evolutionary process of the slope and its route leading to chaos is realized by the bifurcation of period-doublings. Thus, if chaos occurs, it is very difficult to predict a landslide accurately.

Acknowledgements

References

Chau, K.T., 1995. Landslides modeled as bifurcations of creeping slope with nonlinear friction law. Int. J. Solids Struc. 32 (23), 3451–3464.

Chau, K.T., 1998. Applications of catastrophe and bifurcation theories to slope failures. Slope Engineering in Hong Kong, HKIE, Geotechnical Division Annual Seminar (1996–1997 Session), Balkema, Rotterdam, pp. 129–136.

Chau, K.T., 1999. Onset of natural terrain landslides modeled by linear stability analysis of creeping slopes with a two state variable friction law. Int. J. Numer. Anal. Methods Geomech. 23 (15), 1835–1855.

Claes, A., 1996. Application of probabilistic approach in slope stability analyses. Landslides. Balkema, Rotterdam, pp. 1137–1142.

Cui, P., 1991. Experimental study on the mechanism and onset condition of debris flow (in Chinese with English abstract). Science Communication 21, 1650–1652.

Cui, P., Guan, J., 1993. The sudden change properties of debris flow initiation (in Chinese with English abstract). J. Nat. Disas. 2 (1), 53–61.

Duncan, J.M., 1996. State of the art: limit equilibrium and finite element analysis of slope. J. Geotech. Engng. 122 (7), 577–596.

Goodman, R.E., 1989. Introduction to rock mechanics, second ed. University of California at Berkeley, California.

Henley, S., 1976. Catastrophe theory models in geology. Mathema. Geology 8 (6), 649–655.

Homes, P.J., Rand, D.A., 1976. The bifurcations of Duffing's equation: an application of catastrophe theory. J. Sound Vibr. 44, 237–253.

Jaeger, J.C., Cook, N.G.W., 1979. Fundamentals of rock mechanics, third ed. Chapman and Hall, London.

Keilis-Borok, V.I., 1990. The lithosphere of the earth as a nonlinear system with implications for earthquake prediction. Rev. Geophys. 28, 19–34.

Lan, L., 1993. A general limit equilibrium model for three-dimensional slope stability analysis. Cana. Geotech. J. 30, 905–919.

Li, D.H., Huang, Z.Q., 1998. The stochastic resonance and chaos in the evolution of the consequent rock block slope (inclined and vertical) (in Chinese). Chin. Phys. Soc. 47 (3), 380–390.

Liu, B.Z., 1995. Nonlinear dynamics and chaotic basis (in Chinese). Northeastern Teaching University Press, Changchun.

Phillips, J., 1995. Nonlinear dynamics and the evolution of relief. Geomorphology 8 (14), 57–64.

Phillips, J.D., 1992. Nonlinear dynamical systems in geomorphology: revolution or evolution?. Geomorphology 5, 219–229.

Phillips, J.D., 1993. Instability and chaos in hillslope evolution. Am. J. Sci. 293, 25–48.

Qin, S.Q., 2000. Chaotic characteristics of the evolutionary process of slope (in Chinese). Chinese J. Rock Mech. Engng. 19 (4), 486–492.

Qin, S.Q., Jiao, J.J., Wang, S.J., 2000. The predictable time scale of landslide. Bulletin of Engineering Geology and the Environment, in press.

Qin, S.Q., Zhang, Z.Y., Wang, S.T., 1993. An introduction to nonlinear engineering geology (in Chinese). Chinese Southwestern Traffic University Press, Chengdu.

Saunders, P.T., 1980. An introduction to catastrophe theory. Cambridge University Press, London.

Skempton, A.W., 1985. Residual strength of clays in landslides, folded strata and the laboratory. Geotechnique 35, 3–18.

Tang, C.A., 1993. Catastrophe in Rock Unstable Failure (in Chinese). China Coal Industry Publishing House, Beijing.

Tang, C.A., Hudson, J.A., Xu, X., 1993. Rock Failure Instability and Related Aspects of Earthquake Mechanisms (in Chinese). China Coal Industry Publishing House, Beijing.

Thom, R., 1972. Stabilité structurelle et morphogénése. Benjamin, New York.

Yi, C., 1995. A catastrophe model of debris flow (in Chinese). J. Nat. Disas. 4 (2), 53–57.